

# Feature Extraction and Tracking of a Weld Joint for Adaptive Robotic Welding

<sup>1</sup>R.P.Manorathna, P.Phairatt, P.Ogun, T.Widjanarko, M.Chamberlain, L.Justham, S.Marimuthu, M.R.Jackson

EPSRC Centre for Innovative Manufacturing in Intelligent Automation

Wolfson School of Mechanical and Manufacturing Engineering

Loughborough University

Loughborough, LE11 3TU, UK

**Abstract**— Recent advances in automation and sensor technology have enabled the use of industrial robots for complex tasks that require intelligent decision making. Vision sensors have been the most successfully used sensor in many high value industrial applications. Over the recent years, weld seam tracking has been a topic of interest, as most of the existing robotic welding systems operate on basis of pre-programmed instructions. Such automated systems are incapable of adapting to unexpected variations in the seam trajectory or part fit-up. Applications such as tungsten inert gas (TIG) welding of aerospace components require high tolerances and needs intelligent decision making. Such decision making procedure has to be based on the weld groove geometry at any instance. In this study, a novel algorithm along with an automated system was developed for estimating the joint profile and path tracking of a three dimensional (3D) weld groove. A real-time position based closed-loop system was developed with a six axis industrial robot and a laser triangulation based sensor. The system was capable of finding the 3D weld joint profile and position in real-time, and make intelligent decisions accordingly. Raw data from a vision sensor was processed through a novel algorithm to obtain X and Z co-ordinates at an accuracy of 8.3 $\mu$ m and 43 $\mu$ m respectively at an acquisition speed of 2.5 profiles per second. The algorithm was also capable of measuring the weld gaps with an accuracy of 28 $\mu$ m. Finally, the developed system was successfully used for three dimensional seam tracking, and demonstrates an accuracy of  $\pm 0.5$ mm at a tracking speed of 2mm/s.

**Keywords**— Robot, Welding, Intelligence, Tracking, Welding, Laser, Vision

## I. INTRODUCTION

Tungsten inert gas (TIG) welding is an increasingly popular method of metal joining due to its ability to produce high quality welds [1]. Despite the widely recognised merits of the TIG welding process, a negative aspect with it is the shortage of skilled manual welders and more importantly the health and safety concerns associated with arc light, spatter and fumes [1, 2]. Furthermore, the weld quality is closely related to the welders experience or skill, and the repeatability of TIG welding quality cannot be guaranteed with the manual TIG welding process. In order to address these issues, the introduction of an automated TIG weld process is necessary. The study on automation of TIG welding was first initiated in the mid-20<sup>th</sup> century and the first lab trials on robotic welding were carried out in 1970's [2, 3]. Conventional TIG welding robots were mostly successful with flat plates but failed to achieve the desired weld quality [3] with complex parts. Later,

advancement in robots integrated with computers and numerical control (NC) technologies was explored by some researchers. However, the robots continued to fail in achieving the desired weld quality [3] with complex parts. Due to these issues with conventional automation techniques [2], till date most of the TIG welding is performed by manual welders.

A successful TIG welding automation system should be capable enough to adapt for any variations in the weld seam position, caused by part fit-up or distortions. Over the past few decades, extensive number of researches has been carried out on the usage of weld seam tracking. Weld seam tracking is the process of finding the real world coordinates of the weld joint and controlling the welding head accordingly. Various sensors methods such as mechanical, electrical, sonic, magnetic and optical methods was used for seam tracking over the years [4]. With the advancement in imaging techniques, optical seam tracking has shown excellent performance across a wide range of welding processes [3]. Vision sensors are non-contact which makes them independent of the welding process and gather global information such as part fit-up, height mismatch and root gap width.

Among different types of vision sensors, laser scanners are the most widely used in robotic welding due to its high accuracy and robustness at extreme conditions that prevail during the any welding process [5]. Laser scanner operates on the principle of triangulation, which is the process of measuring the pixel coordinates of a point in an image and transform it into the world frame using calibration methods [6].

Although seam tracking has been researched extensively [7-10], not enough work has been carried on finding the geometry of a weld groove. Conventional seam tracking was used only to estimate the weld seam coordinates for path correction of the robots. This process alone could be adequate for a simple geometry, but some advanced applications (e.g. aerospace) requires in-process control of weld parameters [12] to accommodate for complex geometries and part fit-up. Such requirement can only be realized by identification of geometrical features which will enable intelligent decision making and therefore control of the welding process (path and process parameters) [11].

This paper presents an intelligent algorithm which can be used to find joint features and volume to be welded in real-time irrespective of the common weld joint type (U, V or flat groove).

## II. EXPERIMENTAL SETUP AND METHODOLOGY

The experimental setup (Figure 1) consists of a KUKA KR16 six axis industrial robot, a Micro-epsilon laser triangulation based sensor with a lateral accuracy of 20 $\mu$ m, a workstation and an external digital pulse generator (for triggering the laser scanner). Figure 2 shows the arrangement of laser scanner at the end effector of the robot. An industrial computer was used as the central controller for controlling the laser scanner and the robot. The robot and laser scanner were interconnected with the computer through an EtherNet TCP/IP network connection. Stainless steel 316L grade was selected as the work material because it is extensively used in TIG welding. Seam tracking and weld geometry measurements were carried out on a standard V and U-groove profile. The results presented in this paper are only for a V-groove. However, the algorithm functions irrespective of the cross sectional geometry. The detailed geometry of the V-groove is shown in Figure 3.

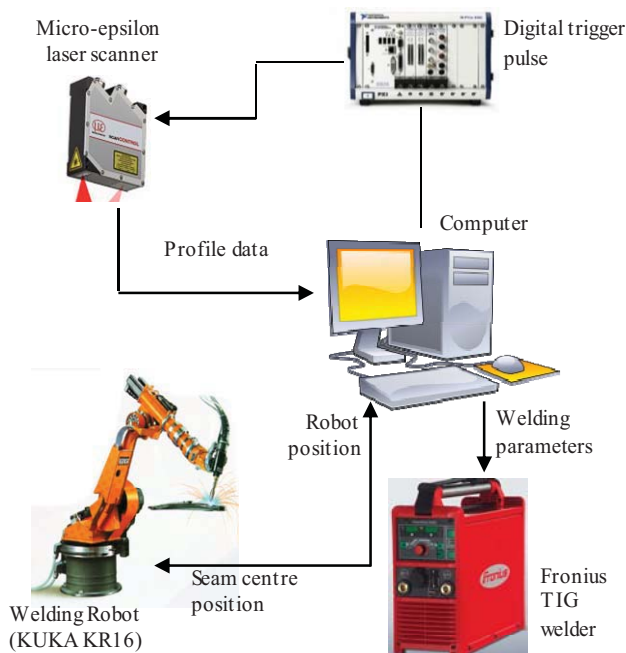


Figure 1. The system integration diagram

A position based control system software was developed to control the overall process in Labview interface. Initially, the robot requests positional data from the computer, which is also used as a command to trigger the laser with a 5V digital pulse. Once triggered, the laser scanner acquires a single profile (two dimensional (2D) data) and sends it to the computer through Ethernet within 20ms. The obtained 2D data is analyzed to find the seam centre which is stored in memory and is used for the tracking-run (as robot positions). Once the center point of the particular profile is calculated, the computer sends a command to the robot, to move to the next position (in this study the robot step is 1mm along the scan direction). After moving to the next position, the robot sends its 3D coordinates back to the

computer which is used again as a command to trigger the laser scanner. The cycle is repeated till the scan is completed.



Figure 2. Laser scanner and the robot



Figure 3. Sample used for the experiments

An algorithm was developed to assess the 2D profile features (points A, B, C and D in Figure 3) such as root gap, and volumetric information of the weld groove at a particular position.

### A. Real-time Feature Detection of 2D profile and Seam Tracking

Figure 4 summarizes the steps involved in detecting the joint features. Point A, B, C and D are identified as the important points to be detected in the joint cross-section.

Raw data obtained from the laser scanner has noise and missing data due to specular reflection. The noise in the raw data needs to be removed prior to data processing. As elucidated in Figure 4(a), most of the noise was observed at the ends of the laser line. This is attributed to the reduced sensitivity of the scanner at the ends of the laser line. Therefore the raw data was cropped by five percent from both ends to remove noisy data which results Figure 4(b).

An edge is defined as a point where there is a sharp change. Hence an edge detection method was used to find points A and D. By calculating the gradient ( $G_i$ ) between each successive laser points (using equation 1), point A and D were recognized. Figure 4(c) shows the obtained gradient values. Start of positive peak is related to point A and fall of negative peak is related point D.

$$G_t = \frac{y_i - y_{i-1}}{x_i - x_{i-1}} \quad (1)$$

$$dx_i = x_i - x_{i-1} \quad (2)$$

where,  $dx$  is the lateral resolution of the sensor and  $x_i$  and  $x_{i-1}$  are  $x$  coordinates of two adjacent laser points.

According to the manufacturer the lateral resolution of the laser scanner is  $20\mu\text{m}$  and it was assumed that the gap between point  $B$  and  $C$  is always more than the sensor resolution. Points  $B$  and  $C$  were established on basis of maximum horizontal offset between two successive laser points. Equation 2 is used between all the adjacent laser points in a single 2D cross sectional profile data which results Figure 4(d). Points  $B$  and  $C$  exists where the spike is detected. Identified points are then used to calculate the coordinates of the middle points of the seam.

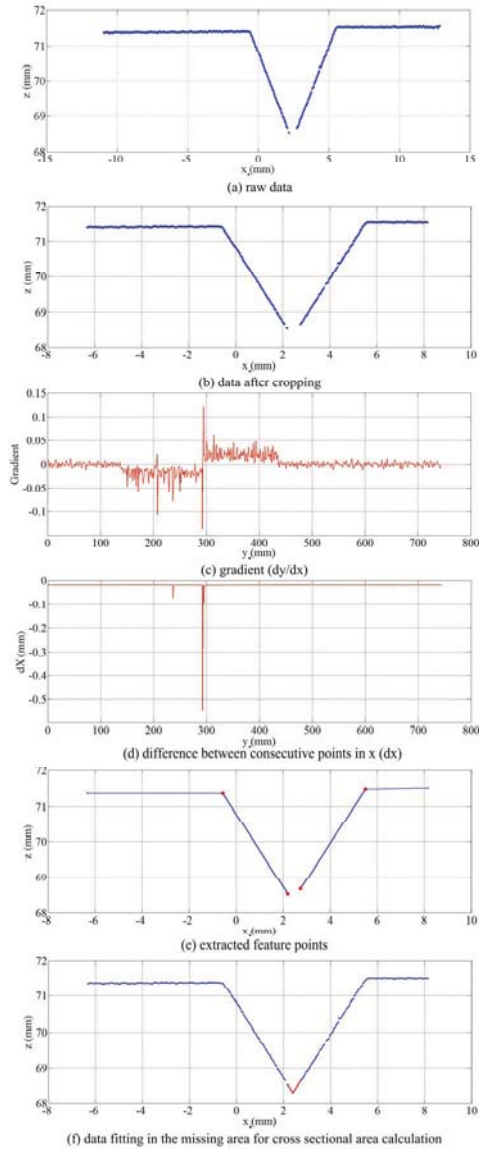


Figure 4. Real-time feature detection algorithm using 2D profiles

Figure 5, shows a cross-sectional view of the weld joint. In order to calculate the area of the V-profile, the missing data between point  $B$  and  $C$  (due to the presence of the physical gap between the parts) needs to be established. This is achieved by calculating the intersection point of line  $AB$  and  $CD$ , and then fitting points at an interval of sensor lateral resolution ( $20\mu\text{m}$ ) from point  $B$  to  $C$  which is shown in Figure 4(f) in red.

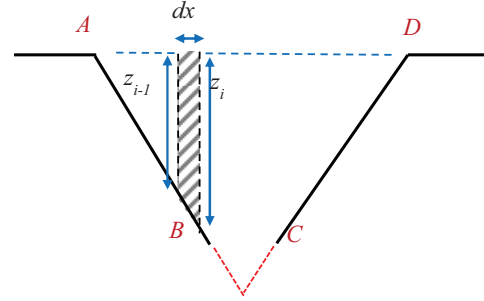


Figure 5. Sectional view of the groove for feature detection

As can be noticed from Figure 5, two consecutive laser points form a trapezoidal elemental area on the joint surface. Also two parallel lines of the trapezoidal element give the respective depth values of the two consecutive laser points. By summing up the area covered by all the trapezoidal elements (from  $A$  to  $D$ ), the total area under a single profile can be calculated using equation 3.

$$\text{Area} = \sum_{i=0}^n (Z_i + Z_{i-1}) \times dx_i / 2 \quad (3)$$

#### B. Post-processing Algorithm for Weld Groove Identification

The surface characteristic (reflectivity) of the weld sample significantly influences the quality and repeatability of the data. Laser scanners tend to produce noisy data if the surface is highly reflective or if there was any change in angle (between the scanning and the surface). Hence a suitable filtering method is vital to account for noise in the data.

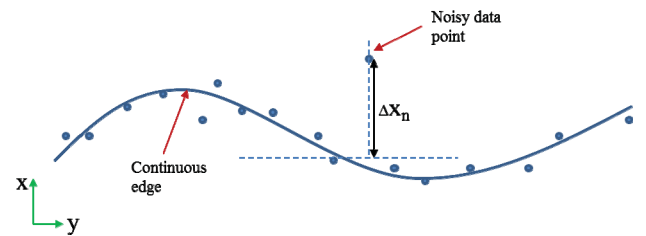


Figure 6. Continuous weld groove edge and detected noisy data point

$$\Delta X_n = X_n - X_{n-1} \quad (4)$$

$$\Delta Y_n = Y_n - Y_{n-1} \quad (5)$$

Figure 6 shows a noisy data point in a 2D path. However, the maximum distance between two consecutive laser points in  $x$  direction ( $\Delta X$ ) should be considerably close to laser scanners' lateral resolution (a well machined weld groove does not have



sudden changes in x-direction). If any point has a significantly higher horizontal offset from its previous point it could be an outlier. Therefore, a threshold value was defined to filter any point which has an offset more than the specified threshold value. This filtering method was used to remove high amplitude outliers in both  $x$  and  $z$  directions respectively. Equation 4 and 5 defines both horizontal and vertical offsets between two consecutive points. Another filter was used on the resulting data which assigns lower weight to outliers in the regression. This filtering method assigns zero weight to data outside six mean absolute deviations which removes all of the noisy data points.

### III. RESULTS AND DISCUSSION

This section describes results obtained using feature detection and seam tracking algorithms. Experiments were carried out to investigate the performance of feature detection and seam tracking algorithms.

#### A. Feature Detection

The raw 3D data obtained from the laser scanner was processed according to the sequence described in section II-A which results Figure 7 (a). As can be seen from the figure, extracted feature points also contain noisy data points. The filtering method described in section II-B was implemented on the raw data which results Figure 7 (b). As seen from the figure, the resulting data has very low noise which is then plotted on the complete 3D raw point cloud data obtained from the laser scanner as shown in Figure 8.

In order to confirm the accuracy of the algorithm, few randomly selected points from the final result were compared against the corresponding raw data points and are given in Table I. Mean square error in the final  $x$ -coordinate is  $8.3\mu\text{m}$  and  $43\mu\text{m}$  in  $z$ -coordinate respectively.

TABLE I. ACCURACY MEASUREMENT OF FEATURE DETECTION ALGORITHM

Point	x coordinate			z coordinate		
	Raw data (mm)	Final result (mm)	Error ( $\mu\text{m}$ )	Raw data (mm)	Final result (mm)	Error ( $\mu\text{m}$ )
1	-3.553	-3.512	-41	63.05	62.98	70
2	1.74	1.739	1	59.71	59.72	-10
3	-0.499	-0.4984	-0.6	60.18	60.21	-30
4	3.893	3.896	-3	63.04	63.05	-10
5	5.674	5.672	2	62.08	62.14	-60
6	0.779	0.777	2	59.48	59.56	-80

#### B. Root Gap Measurement and Seam Tracking

The root gap is measured between point  $B$  and  $C$  (as shown in Figure 3). To estimate the accuracy of the gap measurements, 14 known gaps were set between the samples using a metric feeler gauge in the range from  $0.05\text{mm}$  to  $1\text{mm}$ . The respective set gap was then measured using the developed robotic scanning system. After that the feature detection algorithm was used to find the gap between point  $B$  and  $C$  and the results are shown in Figure 9(a). The average error in weld gap measurement is  $\pm 28\mu\text{m}$ . This result is acceptable because,

the laser scanner's lateral resolution is  $\pm 20\mu\text{m}$  according to the manufacturer.

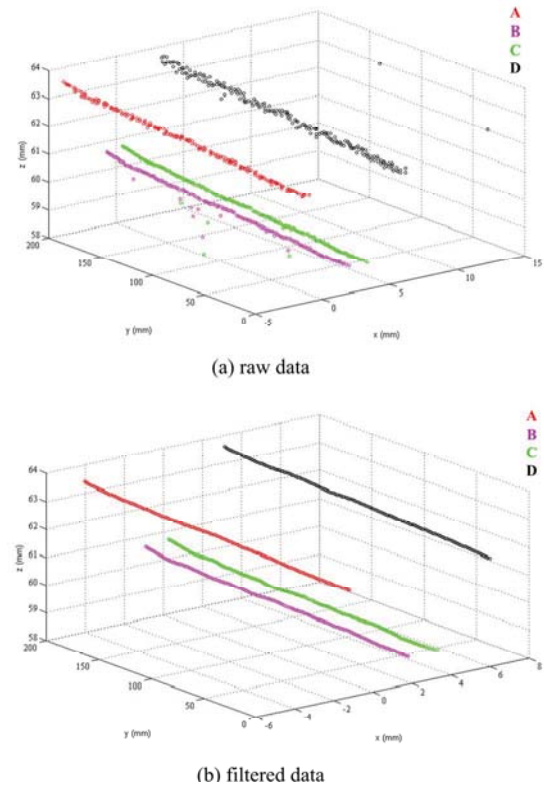


Figure 7. Data processing sequence and results for outlier removal

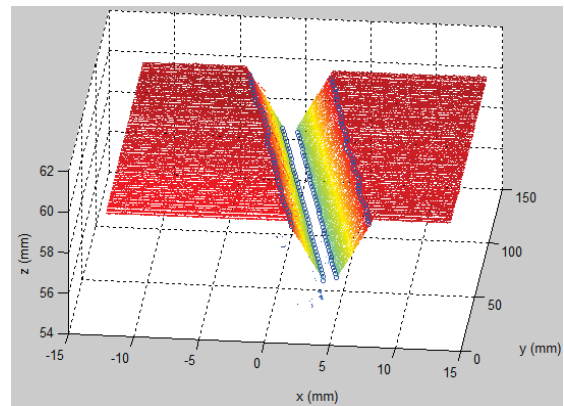


Figure 8. Extracted points on 3D point

Mid-points calculated between  $B$  and  $C$  is used to guide the robot during the tracking-run. In order to assess the accuracy of seam tracking, a test was conducted by setting an angle of  $0.6^\circ$  between the weld seam and the robot travel direction. Figure 9(b) shows the robot path in both scan and tracking runs. Results show that the tracking path makes an angle of  $0.59^\circ$  with the robot path, with an error less than 2%. However, the tracking path has to be linear, since the parts make a linear gap between each other. The standard deviation of the tracked points was found to be  $0.504\text{mm}$ .

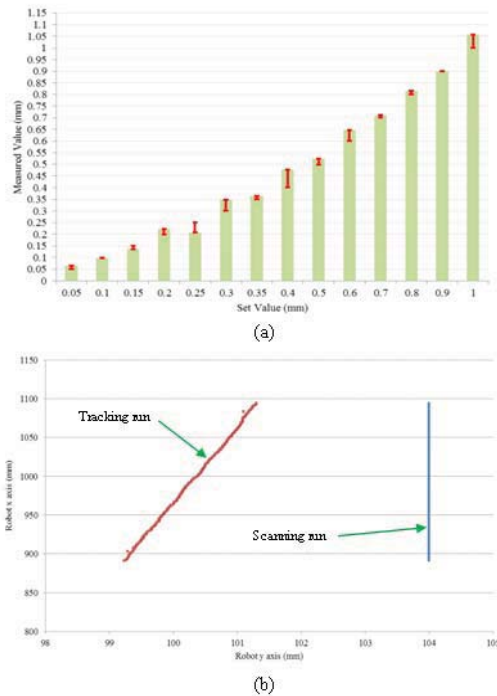


Figure 9. Results on gap measurement and seam tracking

### C. Area Calculation for Parameter Control

In order to check the accuracy of cross sectional area, experiments were carried out on a known cross-sectional area of  $8.64 \text{ mm}^2$ . Figure 10 shows the measured cross sectional area for each profile along the scan direction.

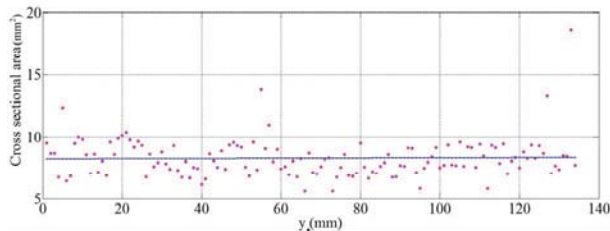


Figure 10. Cross sectional area of the weld profile against weld length

As can be seen from the Figure 10, few points show miscalculated information, which is attributed to the error in finding the feature points. The miscalculated points are eliminated using filtering method (as discussed in section II-B). The mean of resulting area was found to be  $8.51 \text{ mm}^2$ , which gives an accuracy of  $\pm 0.13 \text{ mm}^2$  in area measurements. The standard deviation was found to be  $\pm 0.43 \text{ mm}^2$ , which is acceptable for most welding processes.

## IV. CONCLUSION

This paper successfully presents an algorithm for feature detection of a weld groove with an accuracy of  $8.3 \mu\text{m}$  and

$43 \mu\text{m}$  in  $x$  and  $z$  coordinates respectively. Further, the real-time gap measurement algorithm was able to measure gaps with an accuracy of  $\pm 28 \mu\text{m}$ . The robotic system was able to track a weld seam with a standard deviation of  $0.5 \text{ mm}$  and tracking error of  $1.67\%$  which is acceptable for most welding applications. The algorithm was also able to measure cross sectional area of  $2D$  profiles with a standard deviation of  $0.43 \text{ mm}^2$ . Approximation methods were used to remove outliers from noisy data present in  $2D$  point clouds. The algorithm can be effectively used for adaptive weld process control that needs accurate seam tracking and intelligent decision making for process control. Future work includes improving the system for tracking more complex weld profiles in  $3D$  and carry out robotic TIG welding.

## ACKNOWLEDGEMENT

The authors would like to acknowledge support from the EPSRC Centre for Innovative Manufacturing in Intelligent Automation, in undertaking this research work under grant reference number EP/IO33467/1.

## REFERENCES

- [1] A. B. Earnest, "Automation training for a new work force.," 2014. [Online]. Available: <http://www.thefabricator.com/article/arcwelding/automation-training-for-a-new-work-force>. [Accessed: 05-Mar-2014].
- [2] Esab, "Welding Automation Submerged Arc, TIG, MIG/MAG," Italy, 2011.
- [3] G. Bolmsjö and M. Olsson, "Robotic Arc Welding — Trends and Developments for Higher Autonomy," Lund University, 2001.
- [4] L. W. S.B. Chen, D.B. Zhao, Y.J. Lou, "Computer Vision Sensing and Intelligent Control of Welding Pool Dynamics," Robot. Welding, Intell. Autom., vol. 299, pp. 25–55, 2004.
- [5] P. Julian, Arc Welding Control, 51st ed. China: P. Jiluan, Arc Welding Control. Woodhead Publishing, 2003., 2003.
- [6] N. R. N. A.Ray, Intelligent Seam Tracking for Robotic Welding, 12th ed. Springer Verlag, 1993.
- [7] H. Shen, T. Lin, S. Chen, and L. Li, "Real-Time Seam Tracking Technology of Welding Robot with Visual Sensing," J. Intell. Robot. Syst., vol. 59, no. 3–4, pp. 283–298, Jun. 2010.
- [8] Z. Ye, G. Fang, S. Chen, and M. Dinham, "A robust algorithm for weld seam extraction based on prior knowledge of weld seam," Sens. Rev., vol. 33, no. 2, pp. 125–133, Mar. 2013.
- [9] J. L. J.P.Smith, "A vision-based seam tracker for butt-plate TIG welding," J. Phys., vol. 739, no. 22, 1989.
- [10] H. Ma, S. Wei, Z. Sheng, T. Lin, and S. Chen, "Robot welding seam tracking method based on passive vision for thin plate closed-gap butt welding," Int. J. Adv. Manuf. Technol., vol. 48, no. 9–12, pp. 945–953, Oct. 2009.
- [11] J. N. P. A.Loureiro, G.Bolmsjo, Welding Robots - Technology, System Issues and Application, 17th ed. Springer Verlag, 2006.
- [12] P.C.Miller, In search of smarter welding systems, 60th ed. 1994.